*Desalination and Water Treatment*
www.deswater.com

doi: 10.5004/dwt.2023.29592

297 (2023) 117–130
June

# Development process of graphene field for photocatalytic and antibacterial applications

Jiahe Song[a,b], Jingjing Zhang[c], Kun Zheng[d,*], Zhihua Xu[a,*], Kezhen Qi[a,b,*]

[a]*Hubei Key Laboratory of Industrial Fume and Dust Pollution Control, Jianghan University, Wuhan 430056, China, emails: xuzhihua78@sina.com (Z. Xu), qkzh2003@aliyun.com (K. Qi), songjiahe1998@163.com (J. Song)*
[b]*Institute of Catalysis for Energy and Environment, College of Chemistry and Chemical Engineering, Shenyang Normal University, Shenyang 110034, China*
[c]*College of Pharmacy, Dali University, Dali 671000, China, email: zhjjing22@163.com (J. Zhang)*
[d]*AGH University of Science and Technology, Faculty of Energy and Fuels, Department of Hydrogen Energy, al. A. Mickiewicza 30, 30-059 Krakow, Poland, email: zheng@agh.edu.pl (K. Zheng)*

Received 12 November 2022; Accepted 22 April 2023

## ABSTRACT

As a new type of nanomaterial, graphene (GR) has been widely used in many fields and concerned by researchers. In terms of photocatalysis, graphene and its composites are used in photocatalytic degradation of organic pollutants, photocatalytic water splitting for hydrogen production and photocatalytic reduction of $CO_2$ for $CO_2$ recycling, due to their advantages such as low price and easy availability on the industry side, as well as good photogenerated electron transfer and green environmental protection on the academic side. Furthermore, in the aspect of antibacterial, GR-based nanomaterials have the advantages of stable chemical properties, long-acting time and excellent antibacterial properties, and already show a significant effect in the medical and pharmaceutical fields. Therefore, this review introduces and summarizes the synthesis methods of graphene-based photocatalysts, the application of graphene in the fields of photocatalysis and antibacterial. And the mechanism of graphene participating in the process of photocatalysis, including graphene as cocatalyst, photosensitizer and electron acceptor, is illustrated. Also, the overall views of looking ahead on the future research activities and relating to photocatalysis in this emerging field and possible mechanisms of antibacterial process are elucidated.

*Keywords:* Graphene; Photocatalysis; Antibacterial; $CO_2$ reduction; Water splitting

## 1. Introduction

Novoselov et al. [1], first prepared single-layer graphene (GR) by mechanical separation method from graphite, then graphene began to enter the public's field of vision and was widely used. Graphene has a single layer of carbon atoms with $sp^2$ hybrid orbitals. The valence orbitals of the carbon atoms are composed by three hybrid planar σ orbitals ($sp^2$) forming the plane of GR and a 2p conjugated orbital ($2p_z$) which is perpendicular to the plane of graphene, resulting in formation of a hexagonal thin film in a two-dimensional honeycomb lattice [2]. As the basic constituent unit of fullerenes and carbon nanotubes, graphene also has larger specific surface area, higher chemical stability and better adsorption capacity [3]. This unique structure also makes graphene have excellent optical and electrical properties when used in the field of photocatalysis.

Since Fujishima and Honda [4] discovered the photocatalytic decomposition of water using $TiO_2$ as an electrode in 1972, the applicability of this oxide semiconductor

---

* Corresponding authors.

1944-3994/1944-3986

photocatalyst in solar energy conversion and environmental protection has attracted special attention [5–8]. In general, more semiconductors (such as $TiO_2$ [9], ZnO [10], $WO_3$, CdS [11], $CoFe_2O_4$ [9], BiOCl [12] and g-$C_3N_4$ [13]) can be used as photocatalysts for photocatalytic reactions due to their unique electronic energy band structures. When the photon energy is greater than or equal to the excitation band gap energy ($E_g$) of the semiconductor, electrons in the valence band (VB) of the semiconductor are excited to the conduction band (CB), leaving holes in VB accordingly. These photogenerated holes and photogenerated electrons play an important role in photocatalytic disinfection [14], photocatalytic pollutant degradation [15] and solar energy conversion (including water splitting to hydrogen production and solar photovoltaic power generation) [16,17]. However, the photogenerated electrons and photogenerated holes are unstable and are prone to recombination [18–20]. Their energy is then dissipated in the form of heat or radiation, resulting in lower photocatalytic efficiency.

Graphene-based semiconductor photocatalyst materials have been widely concerned by researchers because of their good conductivity, large specific surface area and high adsorption capacity [21,22]. In the photocatalytic experimental research, graphene as a zero-band gap material cannot be directly used [23], so graphene is usually used in the form of oxidation/reduction graphene in the photocatalytic reaction, or through doping and recombination onto/with other material. In addition, production of defects in graphene, for example, producing graphene nanomesh [24,25], can result in opening the band gap and conducing various photocatalytic applications, for example, near infrared laser stimulation of human neural stem cells into neurons on graphene nanomesh semiconductors [26]. Graphene-based materials have strong adsorption capacity for inorganic and organic molecules due to their unique structure, superior carrier mobility at room temperature and extremely high theoretical specific surface area [27]. Therefore, the effect on degradation of organic pollutants after compounding with other semiconductors is very obvious. Secondly, after graphene is compounded with metal sulfide with excellent hydrogen evolution activity, the efficiency of $H_2$ production from aqueous solution containing sacrificial agent under visible light irradiation is greatly improved [28]. Finally, after proper controlling of the defect density of graphene and the interface contact tightness between graphene and compounded semiconductors, the $CO_2$ adsorption capacity and electronic conductivity of these photocatalysts are significantly increased within a certain range. Therefore, the role of graphene in $CO_2$ reduction is also worthy of further exploration.

Hu et al. [29] have conducted an experimental study on the inhibitory effect of graphene on *Escherichia coli*. Akhavan and Ghaderi [30] also reported on the antibacterial effect and mechanism of the graphene materials, and then the antibacterial research of GR gradually became a hot spot. Graphene nanomaterials inhibit bacteria through light activation, which is controllable and fast. At the same time, compared with ultraviolet active photocatalysts, graphene type visible light active photocatalysts have higher utilization rate of solar energy and lower cost, so they have certain unique potential in medical treatment.

This review first introduces the relevant properties and advantages of graphene nanomaterials and the synthesis methods of graphene-based photocatalysts, then introduces the application of graphene materials in the field of photocatalysis, such as in photocatalytic degradation of organic pollutants, hydrolysis of hydrogen and reduction of $CO_2$. The application of GR in antibacterial field is also reviewed. The possible mechanisms of graphene in the photocatalytic process are proposed, including three possible mechanisms in the antibacterial process by graphene. Finally, we put forward our views on the future research activities related to this emerging field of photocatalysis and antibacterial.

## 2. Synthesis of graphene

Novoselov et al. [1] first reported that GR could be prepared simply through manual mechanical stripping of graphite with just a transparent tape, many reports on graphene synthesis methods have emerged in recent years. Indeed, all of them can be divided into two categories: “down-up” and “top-down” methods. Among “down-up” methods, graphene is mainly synthesized through chemical reactions between atoms or molecules. However, these methods cannot be used for large-scale synthesis because of their complex operation and high costs. Up to now, various graphene materials are usually prepared through “top-down” methods, such as mechanical exfoliation [31], thermal shock exfoliation [32] and electrostatic deposition [33]. Among them, chemical reduction of graphene oxide (GO) is the most commonly used synthesis method, namely the Hummer’s method, as is shown in Fig. 1 [34]. According to this method, firstly, natural graphite powder is oxidized using intensification oxidants (such as nitric acid, potassium permanganate and sulfuric acid) to prepare graphite oxide, and then the GO is obtained through stripping down from the as-prepared graphite oxide. Finally, some aggregates and various inorganic impurities, such as residual ions and acids, are removed by means of centrifugation, washing as well as dialysis [34]. It is worth noting that GO synthesized through chemical oxidation usually contains various oxygen-containing functional surface groups, such as carboxyl, hydroxyl and epoxy functional groups, which can interact with metal cations to provide active sites for the nucleation and growth of nanoparticles, thus promoting the preparation of graphene-based composites.

## 3. Preparation of graphene-based photocatalysts

Many different graphene-based composite photocatalysts have been synthesized via GR together with various semiconductors, which mainly include metal oxides [35], metal sulfur/selenium compounds [36], multi-component metal oxides [37], non-metallic polymers [38] and silver/silver halides [39]. Common preparation methods include the *in-situ* growth [40], solution mixing [41], drop-casting followed by heat-treatment [42] and solvothermal/hydrothermal methods [43].

### 3.1. In-situ growth method

*In-situ* growth is widely used to prepare graphene-metal compound composites. The most common precursors of

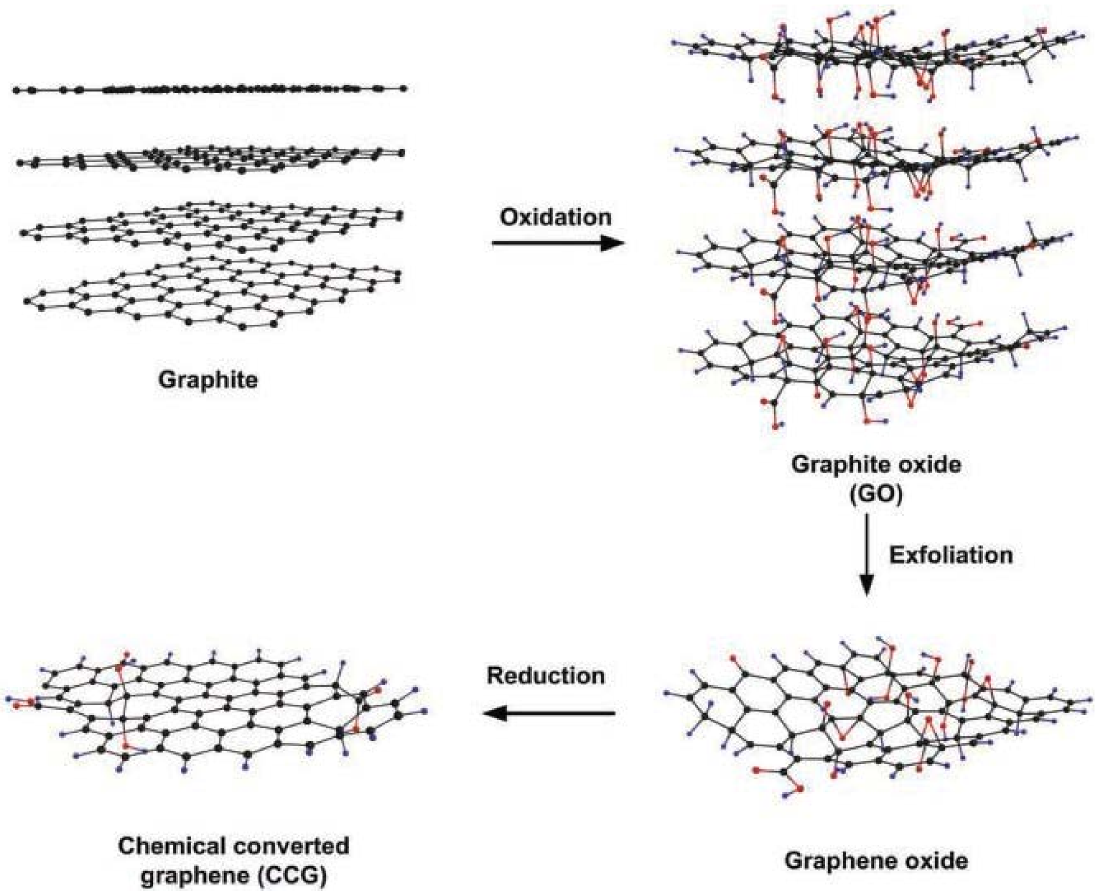

Fig. 1. Graphene oxide is prepared through Hummer's method, and then the chemical converted graphene is prepared via chemical reduction of graphene oxide [34].

graphene and metal compounds are functionalized GO and metal salts, respectively. Generally, the isoelectric point of GO is about pH = 3.9. When GO is dispersed in an aqueous solution with pH = 7, its functionalized surface is negatively charged, and the positively charged metal cations in the solution will be adsorbed on the surface through oxygen of the function groups, which are then converted into corresponding oxides while leaves the GO reduced, forming a rGO/metal compound composite *in-situ*. For example, $Sn^{2+}$ or $Ti^{3+}$ is added to the dispersion of functionalized GO and converted to $SnO_2$ or $TiO_2$ nanoparticles under low-temperature conditions (Fig. 2) [44]. In this process, GO is reduced by $SnCl_2$ or $TiCl_3$ to the reduced graphene oxide (rGO). And since $Sn^{2+}$ and $Ti^{3+}$ have different reduction and hydrolysis capabilities, different morphologies of $SnO_2$ and $TiO_2$ nanocrystals will be emerged simultaneously on the surface of rGO.

Lambert et al. [45] have also reported that $TiF_4$ is hydrolyzed in a GO aqueous dispersion system and flower-like anatase GO/$TiO_2$ composites are synthesized *in-situ*. In this system, when the concentration of graphene oxide is high enough and fully stirred, GO/$TiO_2$ composites with a long range ordered assembly could be obtained. Li et al. [46] have used template free self-assembly method to directly synthesize anatase $TiO_2$ nanospheres with uniform mesopores on graphene sheets. They select titanium sulfate and functional graphene sheets as the starting materials, and take the GR sheets with epoxy and hydroxyl functional groups as the heterogeneous nucleation sites, to fix the as-prepared highly-dispersed mesoporous anatase $TiO_2$ nanospheres on the surface of graphene sheets. In the process of assembling, the orientation of the primary $TiO_2$ nanoparticles promotes the formation of uniform $TiO_2$ nanospheres with single crystal property.

### 3.2. Solution mixing method

Solution mixing method has been widely used to prepare graphene-semiconductor composite photocatalysts. For example, $TiO_2$ particles and GO colloids can be ultrasonically mixed, and then GO can be photocatalytic reduced under ultraviolet radiation to obtain $TiO_2$-graphene composites [47]. And more: Paek et al. [48] used NaOH to hydrolyze $SnCl_4$ to produce $SnO_2$ sol, and then mixed graphene with the above-prepared sol in ethylene glycol to form $SnO_2$-graphene composite. Mukherji et al. [49] synthesized nitrogen-doped $Sr_2Ta_2O_7$-graphene composite by mixing graphene oxide (GO) with nitrogen-doped $Sr_2Ta_2O_7$ ($Sr_2Ta_2O_{7-x}N_x$), and then reducing GO to graphene under xenon lamp light. Zhu et al. [50] synthesized GO-coated Ag/AgX (X = Br, Cl) composites with a water/oil system. After they added the aqueous solution of GO and $AgNO_3$

into the chloroform solution of cetyltrimethylammonium bromide (CTAB) or cetyltrimethylammonium chloride (CTAC), they stirred the mixture magnetically at room temperature to obtain Ag/AgX/GO ternary hybrid composites (Fig. 3). Similarly, graphene, because of its valence bond constructed with the $sp^2$ hybrid carbon network structure, often combines with other graphene-like materials to form large π–π bonds. For example, Sun et al. synthesized a graphene/(graphite-phase carbon nitride) (GR/g-$C_3N_4$) composite polymer photocatalyst through the strategy of straight solution mixing route [51]. The GO prepared through Hummer's method is chemically reduced with hydrazine hydrate in melamine aqueous solution in order to be reduced to graphene. Because the π–π bonds between graphene and melamine aromatic heterocycles is strong, melamine molecules can be absorbed by graphene, and then through condensation polymerization at a high temperature (550°C), the layered g-$C_3N_4$ is generated.

### 3.3. Drop-casting method

Drop-casting method is a method of obtaining a macro GO film by evaporating away the solvent in the GO suspension, as shown in Fig. 4 [52]. The evaporation of the solvent increases the concentration of GO in the suspension, leading to a significant increase in the interaction between the GOs to form a layered nano structure for GO. Of cause, a suitable solvent should not only ensure good dispersion of

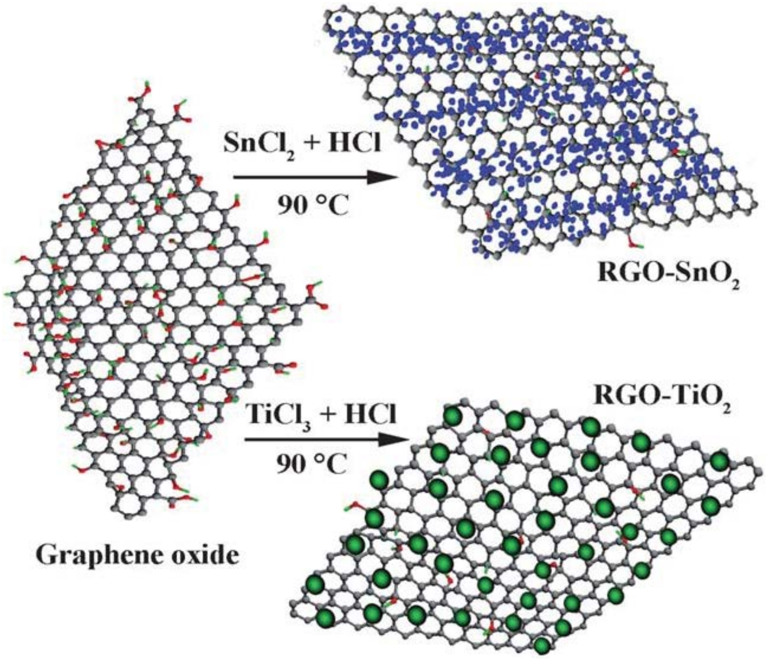

Fig. 2. Schematic diagram of *in-situ* growth mechanism of rGO/$SnO_2$ and rGO/$TiO_2$ [44].

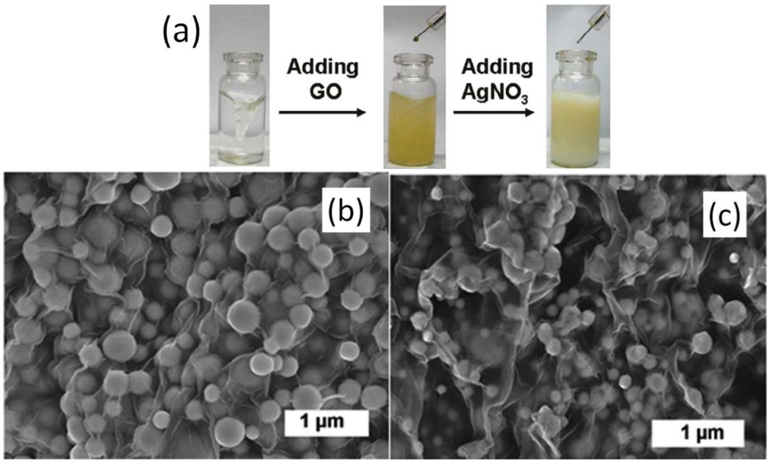

Fig. 3. Schematic diagram of the process of preparing Ag/AgX/GO composites through solution mixing method (a), scanning electron microscopy of Ag/AgBr/GO (b) and Ag/AgCl/GO (c) [49].

GO without rapid precipitation, but also has low boiling point and good volatility. In this case, removing the solvent at an appropriate temperature will ensure the GO in the dispersion to uniformly stack together to form a proper GO film to form a composite material with other components. In short, after proper adjusting the concentration of GO colloidal suspension, the GO suspension is added dropwise or poured onto a specific substrate surface. The substrate can be either a porous support membrane or a carrier with a smooth surface. When standing at room temperature or higher temperature, the solvent in the GO suspension will be vaporized to obtain a layered stacked GO film. The evaporation speed of the solvent has a certain impact on the performance of the membrane. By adjusting the concentration of the GO suspension, the thickness of the composite membrane can be finely controlled. The prepared GO membrane can be used as a functional layer of the composite membrane, or it can also be used as a GO separation membrane.

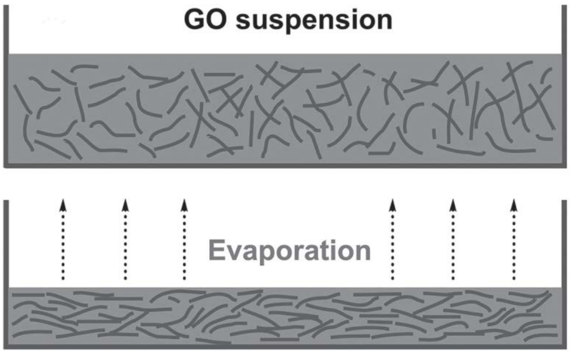

Fig. 4. A proposed self-assembly process of GO film by the evaporation of solvent in GO suspension [51].

### 3.4. Hydrothermal/solvothermal method

Usually, metal compounds are easily soluble in water or organic solvents, and are used as the precursor in the hydrothermal/solvothermal method to produce the corresponding metal oxide crystals. Thus, the corresponding graphene-semiconductor composites can usually be prepared by adding a certain amount of GO in the solvent in advance. For example, since in DMSO solution, the GO surface is negatively charged while $Cd^{2+}$ is positively charged, $Cd^{2+}$ is naturally adsorbed on the GO surface, reacts with $H_2S$ released by DMSO and forms CdS microcrystals on surface of GO sheets, meanwhile under solvothermal reaction conditions, GO is reduced and converted into rGO, as shown in Fig. 5 [53]. Indeed, $H_2S$ released by DMSO is used not only as the reductant of GO, but also as the precursor of sulfide. Therefore, the reduction process of GO and the deposition process of CdS on graphene sheets are carried out simultaneously, so that CdS nanoparticles can uniformly and closely distribute on rGO sheets. In the composite samples, the particle size of CdS nanoparticles is about 10 nm. So, the use of *in-situ* growth method can avoid the agglomeration of CdS nanoparticles on rGO sheets and make them uniformly disperse on the surface of two-dimensional rGO materials, increasing the specific surface area of CdS nanoparticles.

In addition, the morphology of semiconductor nanoparticles on rGO sheets can be controlled through solvothermal method. For example, Chen et al. [54] used a simple

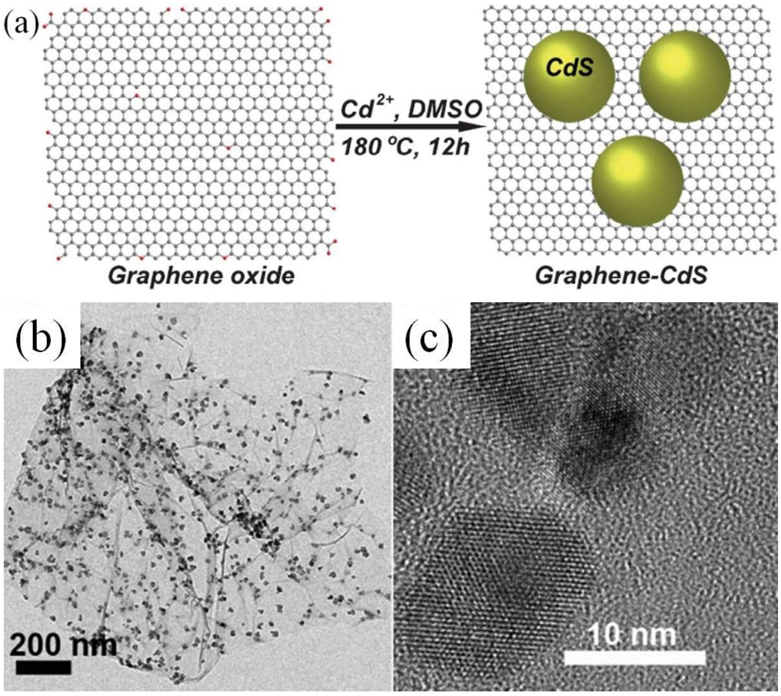

Fig. 5. (a) Scheme of the one-step synthesis of rGO-CdS. (b) Transmission electron microscopy image of a rGO sheet sparsely coated with CdS microcrystals. (c) High-resolution transmission electron microscopy image of CdS crystals on a rGO sheet [52].

solvothermal method to synthesize ultra-thin anatase $TiO_2$ nanosheets with exposed crystal planes of (001), which were dispersed on layered rGO. In this process, anatase $TiO_2$ nanosheets were directly grown on GO, meanwhile GO is transformed into rGO during the heat treatment in the reduction atmosphere of $N_2/H_2$. Thus, they have produced rGO-$TiO_2$ composites with special morphologies and structures. rGO-$TiO_2$ composite photocatalyst can also be synthesized through hydrothermal reaction in ethanol and water solvent with different titanium sources. In order to obtain a homogeneous composite of rGO-semiconductor photocatalyst, recently, Shen et al. [55] reported the one-step solvothermal preparation of rGO-$TiO_2$ composites using glucose as a reducing agent, believing that the preparation method was simple, feasible, easy to operate and environmentally-friendly.

## 4. Application of graphene in photocatalysis

In recent years, the application of photocatalytic technology in energy and environment has shown great potential, and scientists are interested in this research. Among them, the prospective photocatalysts, that is, the composites of two-dimensional graphene-based nanosheet (especially the GO and the rGO nanosheet) with semiconductors, are widely used in different photocatalytic fields, because of their unique functionalized surface structure and interface characteristics, such as energy band structure, charge transport, molecular adsorption and activation ability, which significantly affect the photocatalytic performance of graphene-based photocatalysts. Among them, the more important applications include photocatalytic degradation of pollutants, $H_2$ production and effective reduction of $CO_2$.

In the experiment of removing organic pollutants in sewage treatment, when the band gap of semiconductor photocatalyst is equal to or less than the energy provided by the excitation light source, the electrons on the valence band of the catalyst will jump to the conduction band, so that the photogenerated holes generated on the valence band have strong oxidation property and can oxidize the organic matter into small molecules such as pollution-free $CO_2$ and $H_2O$. At the same time, the photogenerated electrons holding in the conduction band can react with $O_2$ to generate $^{\bullet}OH$ and $^{\bullet}O_2^-$ radical groups which can also be to degrade the pollutants. To reduce the recombination rate of electron–hole pairs, graphene can be combined with semiconductor catalyst forming an electron transport medium, to greatly prolong the lifetime of photogenerated carriers. In addition, graphene can also inhibit the aggregation and growth of semiconductor nanostructures. Moreover, it is also beneficial to improve the specific surface area and photocatalytic activity [56].

In hydrogen production, the electrons and holes generated on the surface of the photocatalyst under the illumination conditions, will move and gather to the surface of the photocatalyst. Electrons accumulated on the CB of semiconductor will combine with $H^+$ in water to produce $H_2$, while the holes remain in the VB of the semiconductor will combine with the $OH^-$ in the water to produce $O_2$. In this way, the sunlight is used to decompose water to produce $H_2$ and $O_2$. The special structure of graphene-based composite provides not only more efficient way to separate electrons and holes, but also generates more effective sites for the holes to be kept the VB of semiconductor to oxidize $OH^-$ in the water to produce $O_2$. At the same time, because of its good conductivity, this composite can replace expensive electrode materials such as metal platinum, so as to produce $H_2$ at low cost and high efficiency. The principle of using photocatalyst to reduce $CO_2$ is similar to that of decomposing water. That is, after electrons and holes are generated on the surface of the catalyst, they will react with $CO_2$ to generate active intermediates such as methoxy ($^{\bullet}OCH_3$) and methyl ($^{\bullet}CH_3$) radicals, which will then be converted into valuable hydrocarbon organic compounds.

### 4.1. Photodegradation of organic pollutants

GR-based composites have many advantages such as excellent electronic conductivity and mobility, high adsorption capacity and high specific surface area. They can be used as a new photocatalyst for degradation of pollutants and environmental improvement. Graphene can improve the performance of common photocatalysts (such as ZnO, $TiO_2$, etc.) to a certain extent, and now it has become an important carbon material [57–59]. A possible mechanism for the photocatalytic gas-phase and liquid-phase degradation of organic pollutants such as benzene and dyes is shown in Fig. 6 [60]. Du et al. [61] prepared $TiO_2$-reduced graphene oxide ($TiO_2$-rGO) thin film with hexagonal two-dimensional structure, and introduced macroporous structure into mesoporous, which increased the specific surface area of the film and greatly improved the photocatalytic activity of $TiO_2$. $TiO_2$-rGO composites have high ability to photodegrade organic dyes and can be used to remove organic pollutants in industrial wastewater. In that study, ordered porous $TiO_2$ films with two-dimensional hexagonal microstructure and good interface connection were successfully prepared. Graphene, as an excellent electron acceptor and electron transport material, was introduced into the mesoporous $TiO_2$ framework. In the mesoporous $TiO_2$-rGO composites, the rGO, as the acceptor of $TiO_2$

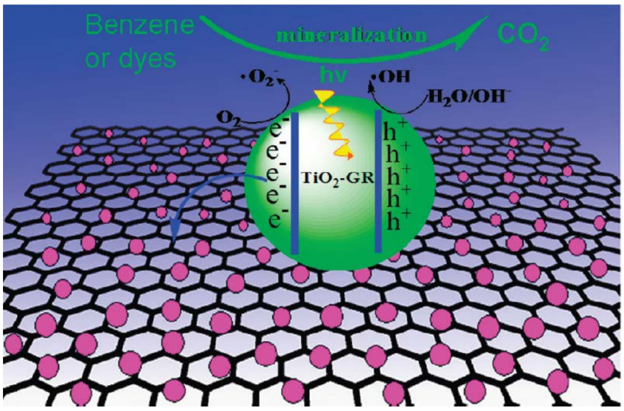

Fig. 6. Proposed mechanism for photocatalytic degradation of organic pollutants (benzene or dyes) over the $TiO_2$-rGO composites in which pink spheres and black sheet represent $TiO_2$ nanoparticles and rGO, respectively (modified from the study of Zhang et al. [59]).

photogenerated electrons, greatly inhibits the photogenerated charge recombination, leaving more photogenerated holes to form reaction species, and promotes the photodegradation of methylene blue. Through investigation of electrochemical impedance spectra, it is found that the introduction of rGO reduces the dielectric frequency, indicating that the resistance of the solid interface layer and the surface charge transfer resistance decrease. Thus, it is verified that the electron acceptor and electron transport characteristics of rGO in $TiO_2$-rGO can inhibit charge recombination and improve its photocatalytic activity.

### *4.2. Hydrogen production*

Hydrogen is widely used in the chemical industry, metallurgical industry, glass production industry, petroleum industry and other fields because of its strong reducibility, flammability and pollution-free combustion products [62]. However, due to the expensive preparation process of hydrogen, scientists are committed to developing a low-cost and simple process for hydrogen production. The method of decomposing water to produce hydrogen by photocatalyst is a hot research topic at present. Fujishima and Honda [4] have found that water can be decomposed by $TiO_2$ photocatalyst to produce hydrogen, and then a large number of methods of producing hydrogen by photocatalyst appeared. Graphene appears in the field of photocatalytic hydrogen production due to its low price and high hydrogen production efficiency. Through the effective doping on and recombination with graphene, the dispersion of photocatalyst can be enhanced, the migration rate of photogenerated charge from the catalyst to water can be accelerated, the carrier pairs recombination probability can be reduced, and the photocatalytic activity of the composite catalyst can be effectively improved [63]. Chang et al. [64] have reported the experimental research on the hydrogen production of rGO (reduced graphene oxide), metal oxide and/or metal sulfide composited rGO. In their study [64], $MoS_2$ as a high-performance noble metal free photocatalyst is used for $H_2$ release under visible light irradiation (Fig. 7). When the mass fraction of $MoS_2$-rGO cocatalyst is 2.0 wt.% and the molar ratio of $MoS_2$-rGO is 1:2, the photocatalytic hydrogen production activity of $MoS_2$-rGO-CdS composite is the highest. This is due to the high activity of $H^+$ ions, adsorbed by S atoms with unsaturated activity on the exposed edge of $MoS_2$, and the photogenerated electrons which can react with $H^+$ directly or migrate through rGO to react with $H^+$ to generate $H_2$. The introduction of rGO enhances the ability of photogenerated charge transfer and inhibits the recombination of electron–hole pairs, thus improving the efficiency of photocatalytic hydrogen evolution. Mou et al. [65] have prepared Eosin Y (EY) sensitized rGO (reduced graphene oxide) (EY-$TiO_2$-rGO). The hydrogen production rate of the EY-$TiO_2$-rGO under visible light and ultraviolet light irradiation is 0.40 and 3.35 mmol/(g·h), respectively, which is three times that of EY-$TiO_2$ under the same conditions. Zhang et al. [66] have reported that the photocatalytic hydrogen production activity of $TiO_2$-GR synthesized by one-step hydrothermal method is 1.6 times that of P25. Wang et al. [67] reported the hydrogen production research of ZnS and graphene composite. The result obtained when the content of the GR in the ZnS-GR composite was 0.1%, the ZnS-GR sample exhibited the highest $H_2$-production rate of 7.42 μmol/h·g, eight times more than the pure ZnS sample. This high visible-light photocatalytic hydrogen production activity is due to the photosensitization of GR. Jia et al. [68] prepared N-graphene/CdS composites and demonstrated to be highly active photocatalysts for hydrogen production under visible light irradiation and the highest photocatalytic activity was found for the sample with a content of 2 wt.% N-graphene doping 210 μmol/h. N-graphene as a cocatalyst can prevent CdS from photocorrosion under light irradiation; N-graphene can be used as a charge collector to promote separation and transfer of photogenerated carriers, and N-graphene can make hydrogen evolution easier and show considerable photocurrent under moderate conditions.

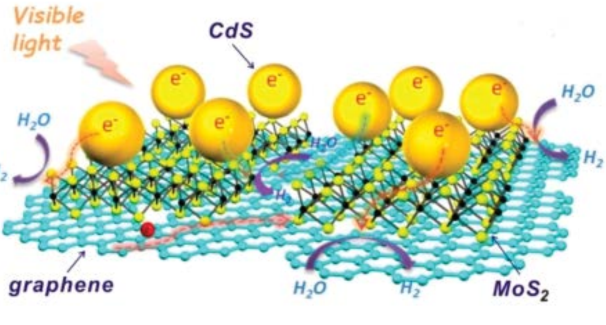

Fig. 7. Schematic diagram of charge transfer in $MoS_2$-rGO-CdS composites under visible light irradiation [63].

In order to improve the activity, the photocatalytic material, such as $TiO_2$, will be in cooperation with other cocatalysts. For example, Xiang et al. [69] have reported that the layered molybdenum sulfide $MoS_2$-rGO composite as a cocatalyst can significantly enhance the photocatalytic activity of $TiO_2$ nanoparticles for hydrogen production. Transmission electron microscopy images show that the $MoS_2$ nanoparticles are dispersed on the rGO sheet, and the $TiO_2$ nanoparticles are evenly distributed on the layered $MoS_2$-rGO composite. The hydrothermal reaction process can closely combine together the three components of $TiO_2$, $MoS_2$ and rGO simultaneously, so as to promote the effective transfer of photogenerated electrons from $TiO_2$ through rGO sheet to $MoS_2$, promote carrier pairs separation, and achieve the purpose of enhancing photocatalytic activity, as shown in Fig. 8. Under the condition of xenon lamp illumination, $MoS_2$-rGO composites with different ratios can improve the photocatalytic hydrogen production activity of $TiO_2$ semiconductor materials; When 0.5% $MoS_2$-rGO composite cocatalyst is added to make $TiO_2$-$MoS_2$-0.5rGO, the photocatalytic decomposition rate of the material reaches the maximum of 165.3 μmol/h. This is mainly because the photogenerated electrons in the $TiO_2$ conduction band can be efficiently transferred through two-dimensional rGO sheet to the $MoS_2$ nanoparticles via the quick electron transport channel of layered graphene, resulting in the promotion of electrons transferred to $MoS_2$ to reduce the adsorbed hydrogen ions and water molecules at $MoS_2$ boundary react to generate hydrogen gas. In fact, the contact of graphene and $MoS_2$ in $MoS_2$-GR composite cocatalyst have synergistic

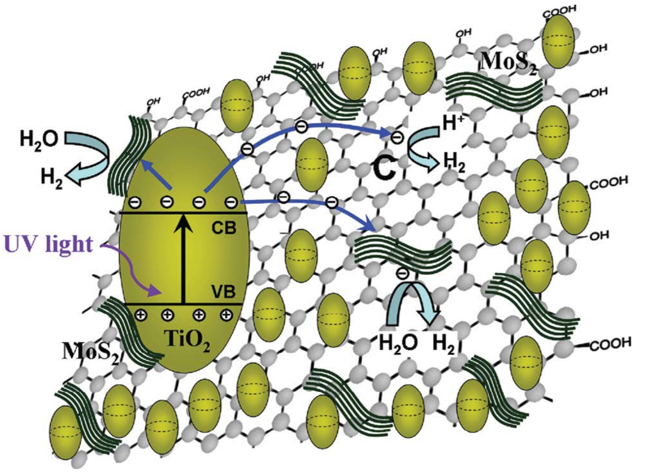

Fig. 8. Schematic diagram of charge migration in $TiO_2$-$MoS_2$-rGO composite [68].

effects, including mainly: reducing carrier pairs recombination, improving carrier transfer rate at the interface, and increasing active adsorption sites and photocatalytic reaction centers as well. In addition, some photogenerated electrons can be directly transferred to $MoS_2$ nanosheets on the surface of $TiO_2$ or carbon atoms of graphene sheets, and these electrons can also directly react with hydrogen ions to generate hydrogen. Therefore, the composite cocatalyst $MoS_2$-rGO synergistically enhances the photocatalytic hydrogen production activity of $TiO_2$, which indicates that graphene as a cocatalyst has a certain application prospect in enhancing the photocatalytic hydrogen production activity.

### *4.3. $CO_2$ reduction*

Coal, oil, natural gas and other fuels are widely used in our lives. The combustion of these fossil fuels will produce a large amount of $CO_2$ and other harmful substances. As the main greenhouse gas, a large amount of $CO_2$ emissions will aggravate the greenhouse effect, and even lead to global warming, glacier melting, sea level rise and other problems, which pose a great threat to the living environment of mankind. At the same time, the carbon element contained in $CO_2$ may be converted into chemical carbon source, to solve the imminent chemical energy crisis. Therefore, in order to reduce the harm of $CO_2$ and the chemical energy crisis, it is necessary to effectively convert it into hydrocarbons. Halmann [70] has first reported in 1978 that $CO_2$ is reduced to HCHO, $CH_3OH$ and HCOOH using GaP as catalyst. The research method for reducing $CO_2$ using photocatalytic technology has begun to enter the public's field of vision. Graphene improves the photocatalytic activity to a certain extent, and the improved photocatalytic efficiency of semiconductors has been applied by researchers into the study of $CO_2$ reduction. Initially, researchers have tested the ability of rGO to photocatalytic reduce $CO_2$ and found that $CO_2$ can be converted to organic hydride (Fig. 9a) [71]. Tu et al. [72] have prepared $TiO_2$-rGO sandwich composite by *in-situ* hydrolysis technology, maintaining the two-dimensional sheet structure of graphene with a transverse dimension of several microns (Fig. 9b). The longer average life and free path of electrons on graphene promote the electrons migrating to cover a larger graphene surface area, thus increasing the possibility of interaction with the adsorbed reactants. When the graphene content is 2.0 wt.%, the total yield reaches the highest value, and the amount of $CH_4$ and $C_2H_6$ produced by reducing $CO_2$ is about 8 and 16.8 μmol/g·h, respectively, of which $C_2H_6$ production is about 2.3 times of that by pure $TiO_2$. Here $CH_4$ and $C_2H_4$ are suggested to be generated by the conversion of methoxy ($^\bullet OCH_3$) and methyl ($^\bullet CH_3$) radicals as reaction intermediates (Fig. 9c). By the way, $^\bullet CH_3$ radicals react with protons and electrons to generate $CH_4$, and two $^\bullet CH_3$ are coupled to generate $C_2H_6$. According to the analysis of the experimental results, the specific surface area of $TiO_2$-rGO is 2.73 times that of commercial P25, which can provide more adsorption sites and reaction centers. Secondly, there are abundant $Ti^{3+}$ sites on the surface of $TiO_2$-rGO. Through the synergistic effect of $Ti^{3+}$ center and graphene, it is more conducive to the transfer electron energy to $CO_2$ to prevent the recombination of electron hole pairs [73].

Organic compound and inorganic compound to build heterojunctions is also an effective way to improve photocatalytic activity [74]. Wang et al. [75] used a simple microwave induced synthesis pathway was explored for *in-situ* growth and assembly of highly dispersed UIO-66-$NH_2$ nanocrystals onto GR, and the formation of highly active photocatalysts for $CO_2$ conversion (Fig. 10). The UIO-66-$NH_2$/GR hybrid thus obtained under visible light irradiation ($\lambda > 410$ nm) exhibits high activity and selectivity in photocatalytic reduction of $CO_2$ to formic acid. The photoreduction efficiency of $CO_2$ in UIO-66-$NH_2$/GR is about 11 times that of pure UIO-66-$NH_2$, which is twice that of traditional hydrothermal synthesis of UIO-66-$NH_2$/GR samples. The proposed microwave assisted synthesis route may generate a large number of "hot spots" (SHS) on the GR surface. These SHS can not only form small UIO-66-$NH_2$ nanocrystals on GR surface, but also have high dispersity, and can greatly improve the interaction between UIO-66-$NH_2$ and GR. This highly dispersed UIO-66-$NH_2$ ultrafine nanocrystal can provide more active surfaces for $CO_2$ capture and enhance light absorption ability, thereby generating photo generated electrons from the UIO-66-$NH_2$ skeleton to reduce $CO_2$ molecules. The powerful UIO-66-$NH_2$/GR interaction can effectively promote the separation of photoelectrons and holes, and inhibit the leaching of UIO-66-$NH_2$ nanoparticles from GR wrap, resulting in high $CO_2$ photoreduction activity and excellent recyclability. This work provides a novel approach for establishing strong interactions between metal–organic frameworks and graphene, with the aim of effectively reducing $CO_2$ under visible light irradiation.

## 5. Application of graphene in treatments antibacterial and germicidal

### *5.1. Antibacterial mechanism of graphene*

The antibacterial effect of graphene on microorganisms is achieved by inhibiting their biological functions. The graphene materiel (GM) will not produce chemical pollution

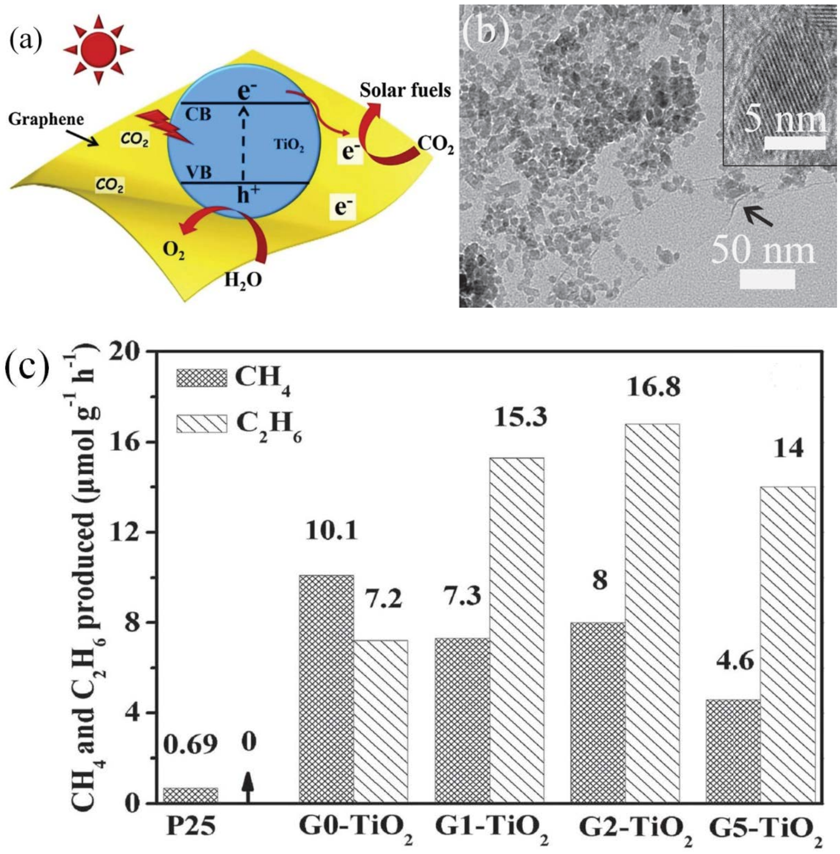

Fig. 9. (a) Schematic illustration of the charge separation and transfer in the $TiO_2$-rGO system and photoreduction of $CO_2$ into solar fuels [70]. (b) Transmission electron microscopy images of rGO/$TiO_2$ composites, (c) photocatalytic $CO_2$ reduction activity of samples $G_x$-$TiO_2$ ($x$ = 0, 1, 2, 5) and P25 [71].

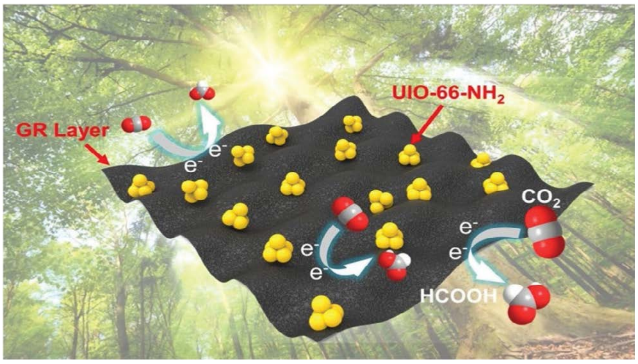

Fig. 10. Photocatalytic mechanism of UIO-66-$NH_2$/GR for reducing $CO_2$ to formic acid [74].

to the environment during the antibacterial process, and has unique advantages of low cost, controllability and high efficiency. In the process of contact with bacteria, the lipid, protein, DNA and RNA in cells all will be damaged by graphene due to the influence of hydrogen bond and electrostatic effect, which will affect the growth and reproduction of microorganisms and eventually lead to inactivation or death of microorganisms [76]. The known antibacterial mechanism of graphene is as follows: (1) physical direct interaction of extremely sharp edges of nanomaterials with cell wall membrane [22], (2) reactive oxygen species (ROS) generation [77] even in dark [78], (3) trapping the bacteria within the aggregated nanomaterials [68], (4) oxidative stress [79], (5) interruption in the glycolysis process of the bacteria [80], (6) DNA damaging [81], and (7) contribution in generation/explosion of nanobubbles [82]. Among these suggested mechanisms, scientists at present have conducted a lot of research on the antibacterial effect of graphene, and there are three more convincing antibacterial mechanisms, including, "Nano-knife" cutting, oxidative stress and wrap bacterial membrane, as shown in Fig. 11 [83].

#### *5.1.1. "Nano-knife" cutting, disturbing cellular components*

Graphene will form sharp edges due to its unique two-dimensional atomic layer structure. This sharp edge is similar to the "nano-knife" that cuts the biological cell membrane or cell wall, destroying its integrity and causing the loss of intercellular substances (such as nucleic acids and proteins). For example: (1) Wang et al. [84] have analyzed the cutting effect of graphene on microorganisms by using dynamic simulation experiments, and proved that graphene can destroy the phospholipid bilayer via transverse cutting by the edge of the layer as a knife. (2) With further research, it is found that the whole nano sheet of GR may be slipped

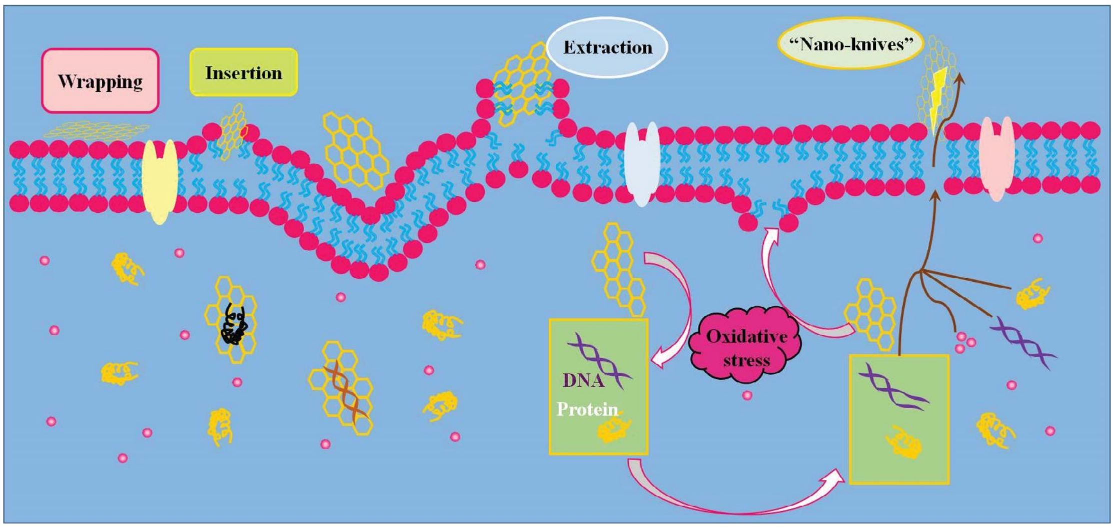

Fig. 11. Three antibacterial mechanisms of graphene [82].

inside the membrane, either keeping parallel in the middle of the lipid bilayer or lying flat on the top of the bilayer. Compared with direct cutting, the insertion of graphene sheets can cause holes in the membrane or turn the phospholipids upside-down. Such changes in the cell membrane will lead to cell death. (3) In addition, graphene sheet may have strong interaction with lipid in the membrane, which exceeds the attraction between lipid molecules in the membrane structure. Thus, graphene sheet will extract lipid molecules from the membrane, damage the integrity of the membrane, and cause cell death [85].

In addition, the direction and angle of contact between graphene and bacteria will affect the sterilization effect. Pham et al. [86] have found that when the cutting angle is 90°, the bactericidal rate is the highest. However, when the angle is 37°, graphene can still effectively kill *Staphylococcus aureus* and *Pseudomonas aeruginosa*. On the other hand, some experimental studies have shown that the antibacterial property of graphene is not determined by the edge cutting of the thin layer, but depends on its base plane. Mangadlao et al. [87] have used LB membrane technology to exclude the bactericidal possibility via physical cutting by graphene oxide, but the results have showed that some *Escherichia coli* are still killed, indicating that graphene has other antibacterial mechanisms.

### 5.1.2. Oxidative stress reaction

The induction of oxidative stress reaction is one of the main mechanisms of graphene toxicity. To activate oxidative stress reaction, the participation of ROS is needed. Once the imbalance between oxidizing agent and antioxidant builds up, the over producing and accumulation of ROS will appear in cells. The ongoing oxidative stress reaction will destroy the basic structure of cells and interfere the basic metabolism of bacteria, thus killing the bacteria. Studies have shown that graphene can absorb oxygen on its defect sites and sheet edges, that can stimulate excessive ROS to be produced in the cells [88–90], resulting in the oxidative stress reaction to take place. That is, from the oxidative stress reaction, excessive superoxide anion, hydroxyl free radical, singlet oxygen and other substances will be produced and accumulated. These substances will affect cell structure, produce peroxidation process with lipids, lead to fatty acid oxidation, stimulate free radical reaction, inhibit the function of mitochondria in cells, inactivate proteins in cells, and may also cause the reduction of intracellular enzyme concentration, inhibit normal metabolism of cells, and eventually induce cells to stop proliferation and die [91,92].

And, the so-called non ROS stress reaction is a process in which important structures or components in cells are damaged by oxidation without ROS production at the first place. Related experiments have shown that graphene may also directly induce oxidative stress reaction without ROS production, that is, it is happening through the non-ROS stress reaction. Liu et al. [93] have tested the levels of superoxide and oxidation in graphene oxide (GO), reduced graphene oxide (rGO) and glutathione, and proved that when the level of superoxide in reaction system itself is not high, the oxidative stress reaction can still be carried out by the charges transferring from cell membrane to graphene, which indicate that GM as rGO can be used as a conductive bridge across the lipid bilayer to transport electrons from intracellular to extracellular in the non-ROS stress process [94].

### 5.1.3. Membrane wrapping the bacteria

It has been observed in all types of cells that the survival of microorganisms depends heavily on the cross-membrane transport, because the cross-membrane transport can input nutrients needed by microorganisms and discharge metabolic wastes. Graphene with specific sp$^2$ hybrid covalent bound is arranged into two-dimensional hexagonal crystal structure by connecting monolayer carbon atoms, and can be formed on the surface of bacteria as an interface barrier to isolate bacteria from their surrounding living environment for almost all nutrients, including $O_2$ and

$CO_2$ molecules. Although GR sheets have some unavoidable defects, which may lead to the passage of some molecules, they are still expected to become an effective barrier for most substances to enter and exit microbial cells [95]. Both experimental and theoretical results show that graphene can block the active sites (such as the transport channels) of the cell membrane, isolate microbial cells from the surrounding environment, and inhibit bacteria proliferation by controlling the input and output of substances [96]. Studies have shown that GR and PVK-GR [(polyvinyl-N-carbazole)-GR] nanocomposites can inhibit the growth and proliferation of gram-positive and gram-negative bacteria by wrapping bacteria [97]. The complete morphology of bacterium itself remains unchanged after being captured and wrapped by graphene, but the cell membrane of bacteria will be affected, and the intracellular activities and basic metabolism will be significantly weakened [98]. Under the scanning electron microscope, it can be observed that the GR sheet will cover and enwind the bacteria after contacting with them, and those cell membrane will be destroyed due to depolarization. It has been also found that graphene nanomaterial with different size will attach to bacterial cell membrane in different patterns. The graphene nano sheet with larger diameter is attached to the cell membrane due to the strong hydrophobic effect of the lipid bilayer, and the GR nano sheet with smaller but better dispersion is easy to attach to the active site on the surface of the cell membrane, which effectively inhibits the growth of bacteria and weakens their viability [99].

### *5.2. Germicidal mechanism of graphene*

GM as the graphene-based nanomaterials can be used in sterilization experiments under the irradiation of visible light or ultraviolet light, that is to say that GM is now involved in photocatalysis. Graphene oxide (GO) is a kernel component of the promising GO based photocatalyst material, possessing good solubility, high specific surface area and many negatively charged active centers. The nanocomposites of GO and semiconductor (GO/semiconductor) are photo active germicides, Hu et al. [29] have reported the germicidal properties of GO for the first time in 2010. An incubation solution with concentration of GO at 85 μg/mL is used as the environment for *Escherichia coli* elimination. After 2 h, the detection shows that the survival rate of bacteria is only 1.5% of the original. After this result was published, it has caused a research upsurge on graphene antibacterial.

Akhavan and Ghaderi [30] have tested the germicidal efficacy of graphene by employing *Escherichia coli* and *Staphylococcus aureus*, and found that graphene had good inhibition effect on both bacteria. Subsequently, graphene as an antibacterial material began to appear widely in the public view. However, due to the unstable antibacterial performance of graphene, and even subject to agglomeration resulting in breeding of bacteria, scientists have compounded graphene with metals or metal oxides to develop nanocomposites with higher antibacterial performance and better stability. Liu et al. [100] have prepared GO Ag composites with good dispersivity. By adsorbing Ag on the GO surface, the probability of contact with bacteria was improved, so the bactericidal rate for *Escherichia coli* reached as high as 99%, which was much higher than that of single GO or Ag nanoparticles. On the other hand, once the metal oxides themselves ($MnO_2$, $TiO_2$, $Fe_3O_4$ and ZnO) are compounded with graphene-based composite materials alone, the synergistic antibacterial performance of the composite will be improved [101–104]. Usually, metal oxide nanoparticles are modified on graphene-based materials by hydrothermal method and solvothermal method. Chella et al. [105] have tested several kinds of bacteria with the composite materials prepared. The bactericidal effect of 100 mg/mL graphene manganese ferrite ($MnFe_2O_4$) solution was the lowest (82%), but still 45% higher than that of single graphene, while the growth of bacteria was completely inhibited in solution of GO-ZnO or GO-$TiO_2$ nanocomposites [102,104]. In addition, the triple antibacterial effect of rGO-CuNPs on *Escherichia coli* and *Staphylococcus aureus* was evaluated. The results showed that the composite had long-term antibacterial effect. An et al. [106] have tested the effect of ZnO-GO nanocomposite on *Escherichia coli* in the experiment, and found that the bacteria contacting ZnO-GO were seriously damaged 2 h later. Jalal et al. [107] and Kavitha et al. [104] both groups have found excellent antibacterial properties of ZnO-GO in experiments. Besides of antibacterial applications, graphene-based nanomaterials in fighting the most challenging viruses and immunogenic disorders [108] and graphene/metal oxide composites have been recently applied in antiviral [109,110] and anti-parasitical purposes [111].

## 6. Conclusion and prospect

In the application of photocatalysis, graphene material has the advantages of strong adsorption capacity, large specific surface area and fast separation speed of photogenerated electron–hole pairs. It can remove pollutants thoroughly during the photocatalytic degradation of organic matter. Meanwhile, it can accelerate the photocatalytic hydrogen production efficiency within a certain period of time when, by doping or fabricating, turning into composite graphene material, and can promote the efficiency of $CO_2$ reduction into effective organic matter too. However, one of the disadvantages of metal oxide/graphene composites is the self-degradation of the graphene content of the composite after many cycles or long-time irradiation (for example, for ZnO [112] and for $TiO_2$ [113]). In this review, the application of graphene-based composite materials in photocatalysis and antibacterial is comprehensively discussed, and the possible mechanism of graphene materials in photocatalysis application is expounded, which indicates certain research direction and provides theoretical basis for the future application of graphene materials in these two aspects. In the application of antibacterial field, the exact role of the proposed antibacterial mechanism includes nano segmentation, oxidative stress reaction and capsule separation.

The mechanism of graphene photocatalytic $CO_2$ reduction needs to be further studied in order to produce specific solar fuels. In addition, it is necessary to systematically compare the role of graphene in photocatalytic $CO_2$ reduction and photocatalytic decomposition of water to hydrogen. Recently, there have been a lot of reports on the research of graphene based photocatalyst for hydrogen production, but the research on graphene based photocatalyst in photocatalytic $CO_2$ reduction is still in its infancy. Comparing the photocatalytic mechanisms of graphene in photocatalytic hydrogen production and in $CO_2$ reduction is helpful, regards to design and prepare graphene-based photocatalysts with high performance. In addition, the theoretical calculation method can simulate the electronic structure characteristics of graphene and its derivatives, which is helpful to understand the semiconductor characteristics and photocatalytic structure-activity relationship of graphene and its derivatives. In-depth study of these mechanisms is expected to make a substantial breakthrough in the production of solar fuel using graphene-based photocatalytic materials.

## Notes

The authors declare no competing financial interest.

## Acknowledgement

This work was supported by the Open Project from Hubei Key Laboratory of Industrial Fume and Dust Pollution Control (HBIK2021-02).

## References

[1] K.S. Novoselov, A.K. Geim, S.V. Morozov, D. Jiang, Y. Zhang, S.V. Dubonos, I.V. Grigorieva, A.A. Firsov, Electric field effect in atomically thin carbon films, Science, 306 (2004) 666–669.

[2] A.K. Geim, K.S. Novoselov, The rise of graphene, Nat. Mater., 6 (2007) 183–191.

[3] F. Schedin, A.K. Geim, S.V. Morozov, E.W. Hill, P. Blake, M.I. Katsnelson, K.S. Novoselov, Detection of individual gas molecules adsorbed on graphene, Nat. Mater., 6 (2007) 652–655.

[4] A. Fujishima, K. Honda, Electrochemical photolysis of water at a semiconductor electrode, Nature, 238 (1972) 37–38.

[5] W. Li, C. Zhuang, Y. Li, C. Gao, W. Jiang, Z. Sun, K. Qi, Anchoring ultra-small $TiO_2$ quantum dots onto ultra-thin and large-sized Mxene nanosheets for highly efficient photocatalytic water splitting, Ceram. Int., 47 (2021) 21769–21776.

[6] K. Qi, C. Zhuang, M. Zhang, P. Gholami, A. Khataee, Sonochemical synthesis of photocatalysts and their applications, J. Mater. Sci. Technol., 123 (2022) 243–256.

[7] K. Qi, R. Selvaraj, T. Al Fahdi, S. Al-Kindy, Y. Kim, G.-C. Wang, C.-W. Tai, M. Sillanpää, Enhanced photocatalytic activity of anatase-$TiO_2$ nanoparticles by fullerene modification: a theoretical and experimental study, Appl. Surf. Sci., 387 (2016) 750–758.

[8] K. Qi, B. Cheng, J. Yu, W. Ho, A review on $TiO_2$-based Z-scheme photocatalysts, Chin. J. Catal., 38 (2017) 1936–1955.

[9] J. Song, J. Zhang, A. Zada, Y. Ma, K. Qi, $CoFe_2O_4/NiFe_2O_4$ S-scheme composite for photocatalytic decomposition of antibiotic contaminants, Ceram. Int., 49 (2023) 12327–12333.

[10] A. Mclaren, T. Valdes-Solis, G. Li, S.C. Tsang, Shape and size effects of ZnO nanocrystals on photocatalytic activity, J. Am. Chem. Soc., 131 (2009) 12540–12541

[11] H. Huang, B. Dai, W. Wang, C. Lu, J. Kou, Y. Ni, L. Wang, Z. Xu, Oriented built-in electric field introduced by surface gradient diffusion doping for enhanced photocatalytic $H_2$ evolution in CdS nanorods, Nano Lett., 17 (2017) 3803–3808.

[12] A. Tadjarodi, O. Akhavan, K. Bijanzad, M.M. Khiavi, Mechanochemically prepared BiOCl nanoplates for removal of rhodamine B and pentachlorophenol, Monatsh. Chem. – Chem. Monthly, 147 (2015) 685–696.

[13] K. Qi, S.-y. Liu, R. Selvaraj, W. Wang, Z. Yan, Comparison of Pt and Ag as co-catalyst on g-$C_3N_4$ for improving photocatalytic activity: experimental and DFT studies, Desal. Water Treat., 153 (2019) 244–252.

[14] K. Qi, X. Xing, A. Zada, M. Li, Q. Wang, S.-y. Liu, H. Lin, G. Wang, Transition metal doped ZnO nanoparticles with enhanced photocatalytic and antibacterial performances: experimental and DFT studies, Ceram. Int., 46 (2020) 1494–1502.

[15] Q. Cui, X. Gu, Y. Zhao, K. Qi, Y. Yan, S-scheme $CuInS_2/ZnS$ heterojunctions for the visible light-driven photocatalytic degradation of tetracycline antibiotic drugs, J. Taiwan Inst. Chem. Eng., 142 (2023) 104679, doi: 10.1016/j.jtice.2023.104679.

[16] K. Qi, Y. Xie, R. Wang, S.-y. Liu, Z. Zhao, Electroless plating Ni-P cocatalyst decorated g-$C_3N_4$ with enhanced photocatalytic water splitting for $H_2$ generation, Appl. Surf. Sci., 466 (2019) 847–853.

[17] K. Qi, S.-y. Liu, Y. Chen, B. Xia, G.-D. Li, A simple post-treatment with urea solution to enhance the photoelectric conversion efficiency for $TiO_2$ dye-sensitized solar cells, Sol. Energy Mater. Sol. Cells, 183 (2018) 193–199.

[18] J. Zhang, Y. Zhao, K. Zhang, A. Zada, K. Qi, Sonocatalytic degradation of tetracycline hydrochloride with $CoFe_2O_4$/g-$C_3N_4$ composite, Ultrason. Sonochem., 94 (2023) 106325, doi: 10.1016/j.ultsonch.2023.106325.

[19] K. Qi, W. Lv, I. Khan, S.-y. Liu, Photocatalytic $H_2$ generation via CoP quantum-dot-modified g-$C_3N_4$ synthesized by electroless plating, Chin. J. Catal., 41 (2020) 114–121.

[20] K. Qi, S.-y. Liu, R. Wang, Z. Chen, R. Selvaraj, Pt/g-$C_3N_4$ composites for photocatalytic $H_2$ production and $^{\bullet}OH$ formation, Desal. Water Treat., 154 (2019) 312–319.

[21] T. Liu, Y. Yang, S. Cao, R. Xiang, L. Zhang, J. Yu, Pore perforation of graphene coupled with *in-situ* growth of $Co_3Se_4$ for high-performance Na-Ion battery, Adv. Mater., 35 (2023) 2207752, doi: 10.1002/adma.202207752.

[22] C. Yang, Y. Wang, J. Yu, S. Cao, Ultrathin 2D/2D graphdiyne/$Bi_2WO_6$ heterojunction for gas-phase $CO_2$ photoreduction, ACS Appl. Energy Mater., 4 (2021) 8734–8738.

[23] Y. Xue, B. Wu, Q. Bao, Y. Liu, Controllable synthesis of doped graphene and its applications, Small, 10 (2014) 2975–2991.

[24] J. Bai, X. Zhong, S. Jiang, Y. Huang, X. Duan, Graphene nanomesh, Nat. Nanotechnol., 5 (2010) 190–194.

[25] O. Akhavan, E. Ghaderi, Graphene nanomesh promises extremely efficient in vivo photothermal therapy, Small, 9 (2013) 3593–3601.

[26] O. Akhavan, E. Ghaderi, S.A. Shirazian, Near infrared laser stimulation of human neural stem cells into neurons on graphene nanomesh semiconductors, Colloids Surf., B, 126 (2015) 313–321.

[27] P. Lazar, F. Karlický, P. Jurečka, M. Kocman, E. Otyepková, K. Šafářová, M. Otyepka, Adsorption of small organic molecules on graphene, J. Am. Chem. Soc., 135 (2013) 6372–6377.

[28] F. Cheng, H. Yin, Q. Xiang, Low-temperature solid-state preparation of ternary CdS/g-$C_3N_4$/CuS nanocomposites for enhanced visible-light photocatalytic $H_2$-production activity, Appl. Surf. Sci., 391 (2017) 432–439.

[29] W. Hu, C. Peng, W. Luo, M. Lv, X. Li, D. Li, Q. Huang, C. Fan, Graphene-based antibacterial paper, ACS Nano, 4 (2010) 4317–4323.

[30] O. Akhavan, E. Ghaderi, Toxicity of graphene and graphene oxide nanowalls against bacteria, ACS Nano, 4 (2010) 5731–5736.

[31] M. Yi, Z. Shen, A review on mechanical exfoliation for the scalable production of graphene, J. Mater. Chem. A, 3 (2015) 11700–11715.

[32] O. Akhavan, The effect of heat treatment on formation of graphene thin films from graphene oxide nanosheets, Carbon, 48 (2010) 509–519.

[33] P. Songkeaw, K. Onlaor, T. Thiwawong, B. Tunhoo, Transparent and flexible humidity sensor based on graphene oxide thin films prepared by electrostatic spray deposition technique, J. Mater. Sci.: Mater. Electron., 31 (2020) 12206–12215.

[34] H. Bai, C. Li, G. Shi, Functional composite materials based on chemically converted graphene, Adv. Mater., 23 (2011) 1089–1115.

[35] E. Rokhsat, O. Akhavan, Improving the photocatalytic activity of graphene oxide/ZnO nanorod films by UV irradiation, Appl. Surf. Sci., 371 (2016) 590–595.

[36] J. Zhang, A. Bifulco, P. Amato, C. Imparato, K. Qi, Copper indium sulfide quantum dots in photocatalysis, J. Colloid Interface Sci., 638 (2023) 193–219.

[37] J. Miao, D. Cai, J. Si, Q. Wang, H. Zhan, Multi-component hierarchical hollow Co–Mo–O nanocages anchored on reduced graphene oxide with strong interfacial interaction for lithium-ion batteries, J. Alloys Compd., 828 (2020) 154379, doi: 10.1016/j.jallcom.2020.154379.

[38] K. Qi, S.-y. Liu, A. Zada, Graphitic carbon nitride, a polymer photocatalyst, J. Taiwan Inst. Chem. Eng., 109 (2020) 111–123.

[39] Y. Chen, P. Wang, Y. Liang, M. Zhao, Y. Jiang, G. Wang, P. Zou, J. Zeng, Y. Zhang, Y. Wang, Fabrication of a three-dimensional porous Z-scheme silver/silver bromide/graphitic carbon nitride@nitrogen-doped graphene aerogel with enhanced visible-light photocatalytic and antibacterial activities, J. Colloid Interface Sci., 536 (2019) 389–398.

[40] J. Hu, Y.-l. Dong, X.-j. Chen, H.-j. Zhang, J.-m. Zheng, Q. Wang, X.-g. Chen, A highly efficient catalyst: *in-situ* growth of Au nanoparticles on graphene oxide–$Fe_3O_4$ nanocomposite support, Chem. Eng. J., 236 (2014) 1–8.

[41] O. Akhavan, Photocatalytic reduction of graphene oxides hybridized by ZnO nanoparticles in ethanol, Carbon, 49 (2011) 11–18.

[42] O. Akhavan, E. Ghaderi, Flash photo stimulation of human neural stem cells on graphene/$TiO_2$ heterojunction for differentiation into neurons, Nanoscale, 5 (2013) 10316–10326.

[43] W.H. Low, P.S. Khiew, S.S. Lim, C.W. Siong, E.R. Ezeigwe, Recent development of mixed transition metal oxide and graphene/mixed transition metal oxide-based hybrid nanostructures for advanced supercapacitors, J. Alloys Compd., 775 (2019) 1324–1356.

[44] J. Zhang, Z. Xiong, X.S. Zhao, Graphene–metal–oxide composites for the degradation of dyes under visible light irradiation, J. Mater. Chem., 21 (2011) 3634–3640.

[45] T.N. Lambert, C.A. Chavez, B. Hernandez-Sanchez, P. Lu, N.S. Bell, A. Ambrosini, T. Friedman, T.J. Boyle, D.R. Wheeler, D.L. Huber, Synthesis and characterization of titania-graphene nanocomposites, J. Phys. Chem. C, 113 (2009) 19812–19823.

[46] N. Li, G. Liu, C. Zhen, F. Li, L. Zhang, H.-M. Cheng, Battery performance and photocatalytic activity of mesoporous anatase $TiO_2$ nanospheres/graphene composites by template-free self-assembly, Adv. Funct. Mater., 21 (2011) 1717–1722.

[47] O. Akhavan, E. Ghaderi, Photocatalytic reduction of graphene oxide nanosheets on $TiO_2$ thin film for photoinactivation of bacteria in solar light irradiation, J. Phys. Chem. C, 113 (2009) 20214–20220.

[48] S.-M. Paek, E. Yoo, I. Honma, Enhanced cyclic performance and lithium storage capacity of $SnO_2$/graphene nanoporous electrodes with three-dimensionally delaminated flexible structure, Nano Lett., 9 (2009) 72–75.

[49] A. Mukherji, B. Seger, G.Q.M. Lu, L. Wang, Nitrogen-doped $Sr_2Ta_2O_7$ coupled with graphene sheets as photocatalysts for increased photocatalytic hydrogen production, ACS Nano, 5 (2011) 3483–3492.

[50] M. Zhu, P. Chen, M. Liu, Graphene oxide enwrapped Ag/AgX (X = Br, Cl) nanocomposite as a highly efficient visible-light plasmonic photocatalyst, ACS Nano, 5 (2011) 4529–4536.

[51] Y. Sun, C. Li, Y. Xu, H. Bai, Z. Yao, G. Shi, Chemically converted graphene as substrate for immobilizing and enhancing the activity of a polymeric catalyst, Chem. Commun., 46 (2010) 4740–4742.

[52] B. Shen, W. Zhai, W. Zheng, Ultrathin flexible graphene film: an excellent thermal conducting material with efficient EMI shielding, Adv. Funct. Mater., 24 (2014) 4542–4548.

[53] A. Cao, Z. Liu, S. Chu, M. Wu, Z. Ye, Z. Cai, Y. Chang, S. Wang, Q. Gong, Y. Liu, A facile one-step method to produce graphene-CdS quantum dot nanocomposites as promising optoelectronic materials, Adv. Mater., 22 (2010) 103–106.

[54] J.S. Chen, Z. Wang, X.C. Dong, P. Chen, X.W. Lou, Graphene-wrapped $TiO_2$ hollow structures with enhanced lithium storage capabilities, Nanoscale, 3 (2011) 2158–2161.

[55] J. Shen, B. Yan, M. Shi, H. Ma, N. Li, M. Ye, One step hydrothermal synthesis of $TiO_2$-reduced graphene oxide sheets, J. Mater. Chem., 21 (2011) 3415–3421.

[56] Q. Li, X. Li, S. Wageh, A.A. Al-Ghamdi, J. Yu, CdS/graphene nanocomposite photocatalysts, Adv. Energy Mater., 5 (2015) 1500010, doi: 10.1002/aenm.201500010.

[57] Y. Yang, H. Tan, B. Cheng, J. Fan, J. Yu, W. Ho, Near-infrared-responsive photocatalysts, Small Methods, 5 (2021) 2001042, doi: 10.1002/smtd.202001042.

[58] Q. Xiang, J. Yu, M. Jaroniec, Graphene-based semiconductor photocatalysts, Chem. Soc. Rev., 41 (2012) 782–796.

[59] L. Zhang, J. Zhang, H. Yu, J. Yu, Emerging S-scheme photocatalyst, Adv. Mater., 34 (2022) 2107668, doi: 10.1002/adma.202107668.

[60] Y. Zhang, Z.-R. Tang, X. Fu, Y.-J. Xu, $TiO_2$-graphene nanocomposites for gas-phase photocatalytic degradation of volatile aromatic pollutant: is $TiO_2$-graphene truly different from other $TiO_2$-carbon composite materials?, ACS Nano, 4 (2010) 7303–7314.

[61] J. Du, X. Lai, N. Yang, J. Zhai, D. Kisailus, F. Su, D. Wang, L. Jiang, Hierarchically ordered macro mesoporous $TiO_2$ graphene composite films: improved mass transfer, reduced charge recombination, and their enhanced photocatalytic activities, ACS Nano, 5 (2011) 590–596.

[62] M. Grätzel, Photoelectrochemical cells, Nature, 414 (2001) 338–344.

[63] H. Zhang, X. Lv, Y. Li, Y. Wang, J. Li, P25-graphene composite as a high performance photocatalyst, ACS Nano, 4 (2010) 380–386.

[64] K. Chang, Z. Mei, T. Wang, Q. Kang, S. Ouyang, J. Ye, $MoS_2$/graphene cocatalyst for efficient photocatalytic $H_2$ evolution under visible light irradiation, ACS Nano, 8 (2014) 7078–7087.

[65] Z. Mou, Y. Dong, S. Li, Y. Du, X. Wang, P. Yang, S. Wang, Eosin Y functionalized graphene for photocatalytic hydrogen production from water, Int. J. Hydrogen Energy, 36 (2011) 8885–8893.

[66] X. Zhang, Y. Sun, X. Cui, Z. Jiang, A green and facile synthesis of $TiO_2$/graphene nanocomposites and their photocatalytic activity for hydrogen evolution, Int. J. Hydrogen Energy, 37 (2012) 811–815.

[67] F. Wang, M. Zheng, C. Zhu, B. Zhang, W. Chen, L. Ma, W. Shen, Visible light photocatalytic $H_2$-production activity of wide band gap ZnS nanoparticles based on the photosensitization of graphene, Nanotechnology, 26 (2015) 345402, doi: 10.1088/0957-4484/26/34/345402.

[68] L. Jia, D.-H. Wang, Y.-X. Huang, A.-W. Xu, H.-Q. Yu, Highly durable N-doped graphene/CdS nanocomposites with enhanced photocatalytic hydrogen evolution from water under visible light irradiation, J. Phys. Chem. C, 115 (2011) 11466–11473.

[69] Q. Xiang, J. Yu, M. Jaroniec, Synergetic effect of $MoS_2$ and graphene as cocatalysts for enhanced photocatalytic $H_2$ production activity of $TiO_2$ nanoparticles, J. Am. Chem. Soc., 134 (2012) 6575–6578.

[70] H. Halmann, Photoelectrochemical reduction of aqueous carbon dioxide on *p*-type gallium phosphide in liquid junction solar cells, Nature, 275 (1978) 115–116.

[71] J. Low, B. Cheng, J. Yu, Surface modification and enhanced photocatalytic $CO_2$ reduction performance of $TiO_2$: a review, Appl. Surf. Sci., 392 (2017) 658–686.

[72] W. Tu, Y. Zhou, Q. Liu, S. Yan, S. Bao, X. Wang, M. Xiao, Z. Zou, An *in-situ* simultaneous reduction-hydrolysis technique for fabrication of $TiO_2$-graphene 2D sandwich-like hybrid nanosheets: graphene-promoted selectivity of photocatalytic-driven hydrogenation and coupling of $CO_2$ into methane and ethane, Adv. Funct. Mater., 23 (2013) 1743–1749.

[73] V.P. Indrakanti, J.D. Kubicki, H.H. Schobert, Photoinduced activation of $CO_2$ on Ti-based heterogeneous catalysts: current state, chemical physics-based insights and outlook, Energy Environ. Sci., 2 (2009) 745–758.

[74] L. Wang, J. Zhang, H. Yu, I.H. Patir, Y. Li, S. Wageh, A.A. Al-Ghamdi, J. Yu, Dynamics of photogenerated charge carriers in inorganic/organic S-scheme heterojunctions, J. Phys. Chem. Lett., 13 (2022) 4695–4700.

[75] X. Wang, X. Zhao, D. Zhang, G. Li, H. Li, Microwave irradiation induced UIO-66-$NH_2$ anchored on graphene with high activity for photocatalytic reduction of $CO_2$, Appl. Catal., B, 228 (2018) 47–53.

[76] J. Li, G. Wang, H. Zhu, M. Zhang, X. Zheng, Z. Di, X. Liu, X. Wang, Antibacterial activity of large-area monolayer graphene film manipulated by charge transfer, Sci. Rep., 4 (2014) 4359, doi: 10.1038/srep04359.

[77] T. Dutta, R. Sarkar, B. Pakhira, S. Ghosh, R. Sarkar, A. Barui, S. Sarkar, ROS generation by reduced graphene oxide (rGO) induced by visible light showing antibacterial activity: comparison with graphene oxide (GO), RSC Adv., 5 (2015) 80192–80195.

[78] V.L. Prasanna, R. Vijayaraghavan, Insight into the mechanism of antibacterial activity of ZnO: surface defects mediated reactive oxygen species even in the dark, Langmuir, 31 (2015) 9155–9162.

[79] A. Ahmad, A. Sattar Qureshi, L. Li, J. Bao, X. Jia, Y. Xu, X. Guo, Antibacterial activity of graphene supported FeAg bimetallic nanocomposites, Colloids Surf., B, 143 (2016) 490–498.

[80] O. Akhavan, E. Ghaderi, *Escherichia coli* bacteria reduce graphene oxide to bactericidal graphene in a self-limiting manner, Carbon, 50 (2012) 1853–1860.

[81] O. Akhavan, E. Ghaderi, A. Akhavan, Size-dependent genotoxicity of graphene nanoplatelets in human stem cells, Biomaterials, 33 (2012) 8017–8025.

[82] M. Jannesari, O. Akhavan, H.R. Madaah Hosseini, B. Bakhshi, Graphene/CuO$_2$ nanoshuttles with controllable release of oxygen nanobubbles promoting interruption of bacterial respiration, ACS Appl. Mater. Interfaces, 12 (2020) 35813–35825.

[83] X. Zou, L. Zhang, Z. Wang, Y. Luo, Mechanisms of the antimicrobial activities of graphene materials, J. Am. Chem. Soc., 138 (2016) 2064–2077.

[84] J. Wang, Y. Wei, X. Shi, H. Gao, Cellular entry of graphene nanosheets: the role of thickness, oxidation and surface adsorption, RSC Adv., 3 (2013) 15776–15782.

[85] R. Guo, J. Mao, L.-T. Yan, Computer simulation of cell entry of graphene nanosheet, Biomaterials, 34 (2013) 4296–4301.

[86] V.T.H. Pham, V.K. Truong, M.D.J. Quinn, S.M. Notley, Y. Guo, V.A. Baulin, M.A. Kobaisi, R.J. Crawford, E.P. Ivanova, Graphene induces formation of pores that kill spherical and rod-shaped bacteria, ACS Nano, 9 (2015) 8458–8467.

[87] J.D. Mangadlao, C.M. Santos, M.J.L. Felipe, A.C.C. de Leon, D.F. Rodrigues, R.C. Advincula, On the antibacterial mechanism of graphene oxide (GO) Langmuir–Blodgett films, Chem. Commun., 51 (2015) 2886–2889.

[88] F. Perreault, A.F. de Faria, S. Nejati, M. Elimelech, Antimicrobial properties of graphene oxide nanosheets: why size matters, ACS Nano, 9 (2015) 7226–7236.

[89] X. Liu, S. Sen, J. Liu, I. Kulaots, D. Geohegan, A. Kane, A.A. Puretzky, C.M. Rouleau, K.L. More, G.T.R. Palmore, R.H. Hurt, Antioxidant deactivation on graphenic nanocarbon surfaces, Small, 7 (2011) 2775–2785.

[90] F. Perreault, A. Fonseca de Faria, M. Elimelech, Environmental applications of graphene-based nanomaterials, Chem. Soc. Rev., 44 (2015) 5861–5896.

[91] L. Shi, J. Chen, L. Teng, L. Wang, G. Zhu, S. Liu, Z. Luo, X. Shi, Y. Wang, L. Ren, The antibacterial applications of graphene and its derivatives, Small, 12 (2016) 4165–4184.

[92] S.C. Smith, D.F. Rodrigues, Carbon-based nanomaterials for removal of chemical and biological contaminants from water: a review of mechanisms and applications, Carbon, 91 (2015) 122–143.

[93] S. Liu, T.H. Zeng, M. Hofmann, E. Burcombe, J. Wei, R. Jiang, J. Kong, Y. Chen, Antibacterial activity of graphite, graphite oxide, graphene oxide, and reduced graphene oxide: membrane and oxidative stress, ACS Nano, 5 (2011) 6971–6980.

[94] J. Chen, X. Wang, H. Han, A new function of graphene oxide emerges: inactivating phytopathogenic bacterium *Xanthomonas oryzae pv. Oryzae*, J. Nanopart. Res., 15 (2013) 1658, doi: 10.1007/s11051-013-1658-6.

[95] S. Liu, M. Hu, T.H. Zeng, R. Wu, R. Jiang, J. Wei, L. Wang, J. Kong, Y. Chen, Lateral dimension-dependent antibacterial activity of graphene oxide sheets, Langmuir, 28 (2012) 12364–12372.

[96] O. Akhavan, E. Ghaderi, A. Esfandiar, Wrapping bacteria by graphene nanosheets for isolation from environment, reactivation by sonication, and inactivation by near-infrared irradiation, J. Phys. Chem. B, 115 (2011) 6279–6288.

[97] I.E. Mejías Carpio, C.M. Santos, X. Wei, D.F. Rodrigues, Toxicity of a polymer–graphene oxide composite against bacterial planktonic cells, biofilms, and mammalian cells, Nanoscale, 4 (2012) 4746–4756.

[98] J. Chen, H. Peng, X. Wang, F. Shao, Z. Yuan, H. Han, Graphene oxide exhibits broad-spectrum antimicrobial activity against bacterial phytopathogens and fungal conidia by intertwining and membrane perturbation, Nanoscale, 6 (2014) 1879–1889.

[99] M. Dallavalle, M. Calvaresi, A. Bottoni, M. Melle-Franco, F. Zerbetto, Graphene can wreak havoc with cell membranes, ACS Appl. Mater. Interfaces, 7 (2015) 4406–4414.

[100] L. Liu, J. Liu, Y. Wang, X. Yan, D.D. Sun, Facile synthesis of monodispersed silver nanoparticles on graphene oxide sheets with enhanced antibacterial activity, New J. Chem., 35 (2011) 1418–1423.

[101] S. Cao, C. Chen, J. Zhang, C. Zhang, W. Yu, B. Liang, Y. Tsang, MnO$_x$ quantum dots decorated reduced graphene oxide/TiO$_2$ nanohybrids for enhanced activity by a UV pre-catalytic microwave method, Appl. Catal., B, 176–177 (2015) 500–512.

[102] Y.-N. Chang, X.-M. Ou, G.-M. Zeng, J.-L. Gong, C.-H. Deng, Y. Jiang, J. Liang, G.-Q. Yuan, H.-Y. Liu, X. He, Synthesis of magnetic graphene oxide–TiO$_2$ and their antibacterial properties under solar irradiation, Appl. Surf. Sci., 343 (2015) 1–10.

[103] C.-H. Deng, J.-L. Gong, G.-M. Zeng, C.-G. Niu, Q.-Y. Niu, W. Zhang, H.-Y. Liu, Inactivation performance and mechanism of *Escherichia coli* in aqueous system exposed to iron oxide loaded graphene nanocomposites, J. Hazard. Mater., 276 (2014) 66–76.

[104] T. Kavitha, A.I. Gopalan, K.-P. Lee, S.-Y. Park, Glucose sensing, photocatalytic and antibacterial properties of graphene–ZnO nanoparticle hybrids, Carbon, 50 (2012) 2994–3000.

[105] S. Chella, P. Kollu, E.V.P.R. Komarala, S. Doshi, M. Saranya, S. Felix, R. Ramachandran, P. Saravanan, V.L. Koneru, V. Venugopal, S.K. Jeong, A. Nirmala Grace, Solvothermal synthesis of MnFe$_2$O$_4$-graphene composite—investigation of its adsorption and antimicrobial properties, Appl. Surf. Sci., 327 (2015) 27–36.

[106] S.S. An, K.-S. Yun, L. Zhong, Graphene oxide-modified ZnO particles: synthesis, characterization, and antibacterial properties, Int. J. Nanomed., 10 (2015) 79–92.

[107] R. Jalal, E.K. Goharshadi, M. Abareshi, M. Moosavi, A. Yousefi, P. Nancarrow, ZnO nanofluids: green synthesis, characterization, and antibacterial activity, Mater. Chem. Phys., 121 (2010) 198–201.

[108] T. Seifi, A. Reza Kamali, Antiviral performance of graphene-based materials with emphasis on COVID-19: a review, Med. Drug Discovery, 11 (2021) 100099, doi: 10.1016/j.medidd.2021.100099.

[109] O. Akhavan, M. Choobtashani, E. Ghaderi, Protein degradation and RNA efflux of viruses photocatalyzed by graphene-tungsten oxide composite under visible light irradiation, J. Phys. Chem. C, 116 (2012) 9653–9659.

[110] J. Prakash, S.B.N. Krishna, P. Kumar, V. Kumar, K.S. Ghosh, H.C. Swart, S. Bellucci, J. Cho, Recent advances on metal oxide based nano-photocatalysts as potential antibacterial and antiviral agents, Catalysts, 12 (2022) 1047, doi: 10.3390/catal12091047.

[111] O. Akhavan, E. Ghaderi, K. Rahimi, Adverse effects of graphene incorporated in TiO$_2$ photocatalyst on minuscule animals under solar light irradiation, J. Mater. Chem., 22 (2012) 23260–23266.

[112] O. Akhavan, Graphene nanomesh by ZnO nanorod photocatalysts, ACS Nano, 4 (2010) 4174–4180.

[113] O. Akhavan, M. Abdolahad, A. Esfandiar, M. Mohatashamifar, Photodegradation of graphene oxide sheets by TiO$_2$ nanoparticles after a photocatalytic reduction, J. Phys. Chem. C, 114 (2010) 12955–12959.